Seasonal variability of zooplankton size spectra at Mombetsu Harbour in the southern Okhotsk Sea during 2011: an analysis using an optical plankton counter

Hikaru Hikichi[a,*], Daichi Arima[a], Yoshiyuki Abe[a], Kohei Matsuno[a,b], Soshi Hamaoka[c], Seiji Katakura[c], Hiromi Kasai[d], Atsushi Yamaguchi[a]

a Laboratory of Marine Biology, Graduate School of Fisheries Science, Hokkaido University, 3-1-1 Minato-cho, Hakodate, Hokkaido 041-0821, Japan

b Australian Antarctic Division, 203 Channel Highway, Kingston, Tasmania 7050, Australia

c Kaiyo-Koryukan, Kaiyo-Koen 1, Mombetsu, Hokkaido 094-0031, Japan

d Hokkaido National Fisheries Research Institute, Japan Fisheries Research and Education Agency, 116 Katsurakoi, Kushiro, Hokkaido 085-0802, Japan

*Corresponding author

E-mail address: h.hikichi@fish.hokudai.ac.jp (H. Hikichi)

Abstract

To evaluate the temporal changes in zooplankton size spectra, optical plankton counter (OPC) measurements were made of high-frequency time-series zooplankton samples collected at approximately 3.5-day intervals in Mombetsu Harbour, which is located in the southern Okhotsk Sea, from January to December 2011. Based on biomasses of 47 equivalent spherical diameter (ESD) size classes binned at 0.1 mm intervals across 0.35-5 mm, the Bray-Curtis similarity index separated the zooplankton community into six groups (A-F). The occurrence of each group was separated seasonally. Thus, groups A and B were observed during the ice-covered season and summer season, respectively. During March and June, groups C-F were observed. Their occurrence varied in the short term in relation to the exchange of water masses. Groups A and C, which were observed from January to April, showed flatter normalized biomass size spectra (NBSS) slopes (–0.85 - –1.1), which indicate low productivity. In contrast, the other groups showed steeper slopes (–1.31 - –1.52) from May to December, with high productivity. Throughout the year, the frequency of highly productive groups occurred at a high level (95.2%). Although the seasonal variability in zooplankton size and productivity in Mombetsu Harbour was mainly governed by water

mass exchanges, the productivity was continuously high throughout nearly all of the one-year study period.

1. Introduction

From a fishery standpoint, information on the zooplankton size spectrum is highly important. The zooplankton size spectrum affects the fish growth and mortality rates (van de Meeren and Næss, 1993). From the oceanography perspective, zooplankton size affects the vertical material transport, also termed the “biological pump” (Michaels and Silver, 1988; Docklow et al., 2001). Thus, information on the zooplankton size spectrum is important for both fisheries and oceanography. However, size measurements on zooplankton communities using microscopic observation are time-consuming. To overcome this problem, Herman (1988) developed an optical plankton counter (OPC) that measures the zooplankton size and number quickly and accurately, and it has been applied in various marine ecosystems (Zhou et al., 2009; Matsuno et al., 2012). The size structure of zooplankton roughly reflects the taxonomic composition. OPCs have the capability to identify or separate species or specific groups in a limited way (Herman and Harvey, 2006), but it is difficult to identify the zooplankton taxonomic composition within the same size range. To clarify which zooplankton are present and contribute to zooplankton production, the taxonomic composition of the sample is needed.

Normalized biomass size spectra (NBSS) analysis of zooplankton

size-spectrum data from OPC measurements has been used to evaluate the marine ecosystem structure in many locations around the world (Basedow et al., 2010; Matsuno et al., 2012; Sato et al., 2015). NBSS is known to be an index of productivity of marine ecosystems, transfer efficiency to higher trophic levels and predator-prey interactions (Herman and Harvey, 2006; Zhou, 2006). The slope of NBSS at approximately -1 indicates a theoretical steady state (Sprules and Munawar, 1986). In general, slopes steeper than -1 indicate bottom-up control (Moore and Suthers, 2006) or high productivity with low transfer efficiency (Sprules and Munawar, 1986; Zhou, 2006). Slopes flatter than -1 indicate top-down control (Moore and Suthers, 2006) or low productivity with high transfer efficiency (Sprules and Munawar, 1986; Zhou, 2006). However, little information is available on the zooplankton size spectra in the Okhotsk Sea. Additionally, limited information is available for the southern regions during the summer (Sato et al., 2015).

In the southern Okhotsk Sea, owing to the differences in tidal levels between the Okhotsk Sea and the Japan Sea, inflow amounts from the East Sakhalin Current and Soya Warm Current are known to be balanced (Aota, 1975) (Fig. 1a). The Soya Warm Current increases after the ice melt season and is high during autumn, whereas it is at its lowest during winter (Fukamachi et al., 2008). The Okhotsk Sea is the southernmost

69 ice-covered ocean in the Northern Hemisphere, and pack ice is transported from the
70 northern area from January to February (Hiwatari et al., 2008). Once the ice has
71 melted, an ice edge bloom is initiated (Mustapha and Saitoh, 2008). The decrease in
72 sea ice may also be an important factor in initiating phytoplankton blooms (Kasai et al.,
73 2017). Thus, the physical condition of the southern Okhotsk Sea is characterized by
74 the large seasonal changes caused by the East Sakhalin Current and the Soya Warm
75 Current. The zooplankton community also varies between the currents (Asami et al.,
76 2007), which suggests that temporal changes in the hydrological environment, including
77 water masses, affect the NBSS of zooplankton communities. Despite their importance,
78 little information is available on the temporal changes in the zooplankton size spectra in
79 this region.

80 In the present study, the temporal changes in the zooplankton size spectra at
81 Mombetsu Harbour in the southern Okhotsk Sea were studied by using OPC
82 measurements of zooplankton samples collected at fine temporal intervals
83 (approximately every 3.5 days) from January to December 2011. Based on the OPC
84 data, an NBSS analysis was conducted. To evaluate the environmental factors
85 governing the zooplankton size spectra, structural equation modelling (SEM) analysis
86 was also performed. Regional comparisons were made between the NBSS slopes and

87 characteristics of the zooplankton community at Mombetsu Harbour in the southern
88 Okhotsk Sea.

89 **2. Methods**

90 *2.1. Field Sampling*

91 Zooplankton sampling was conducted from a bridge across a pier at a depth of
92 9 m in Mombetsu Harbour (Fig. 1b). Vertical hauls with a NORPAC net (mouth
93 diameter 45 cm, mesh size 335 μm) were made from an 8 m depth to the sea surface.
94 Sampling was conducted during the daytime at intervals of 3-4 days (105 sampling
95 times) from January 2 to December 31, 2011. Zooplankton samples were preserved
96 with 5% borax-buffered formalin seawater. Temperature and salinity were measured
97 by Conductivity Temperature Depth profiler (CTD) (JFE Advantec, ASTD102).
98 Surface seawater samples were collected with a bucket, frozen and used for nutrient
99 (NO_3) measurement by an AutoAnalyzer (Bran+Luebbe, AACS). A portion of each
100 seawater sample was filtered through GF/F filters, and chlorophyll a (Chl. *a*) was
101 extracted in *N*,*N*-dimethylformamide and measured by a fluorometer (Turner Designs,
102 10AU). As with the other environmental data, the meteorological data (rainfall,
103 maximum wind speed) at Mombetsu were downloaded from the website of the

104 Meteorological Agency (http://www.data.jma.go.jp/obd/stats/etrn/index.php), and tidal
105 level data at Mombetsu were obtained from the J-DOSS website
106 (http://www.jodc.go.jp/jodcweb/JDOSS/index_j.html).

107 *2.2. OPC analysis*

108 Zooplankton samples, preserved with 5% borax-buffered formalin seawater,
109 were used for OPC (Model OPC-1L: Focal Technologies Crop.) measurements using a
110 flow-through system (CT&C Co. Ltd., Tokyo, Japan). OPC measurements were made
111 following the procedures outlined by Yokoi et al. (2008) as follows: (1) low flow rate
112 (approximately 10 L min^{-1}), (2) low particle density (<10 counts sec^{-1}) and (3)
113 measurement taken only once without staining. Because OPC cannot separately count
114 the zooplankton and non-zooplankton particles, the count data can include
115 non-zooplankton (e.g., copepod fragments and detritus), especially in the small size
116 classes. In this study, the size classes smaller than the mesh size of the net (335 μm)
117 were removed from analysis because the particle counts in the smaller size classes could
118 be non-quantitative and/or underestimated. Size classes larger than 5.00 mm were also
119 removed because these particles were often assemblages of zooplankton (e.g., medusa
120 fragments combined the other zooplankton), which was visually confirmed during OPC

measurement.

From the number of particles (n), filtered volume of the net (F: m^3) and vertical haul depth (8 m), the abundance (N: ind. m^{-2}) at 4,096 equivalent spherical diameter (ESD) size categories was calculated from the following equation:

$$N = \frac{n \times 8}{F}$$

The biovolume of the zooplankton community at 4,096 ESD size categories (mm^3 $ind.^{-1}$) was calculated from the ESD. By multiplying the abundance at each size category (N) (ind. m^{-2}), the biovolume (mm^3 m^{-2}) was calculated.

Additionally, we measured the size spectra of the dominant species using sorted samples with up to 100 individuals (24 individuals for *Neocalanus cristatus*).

2.3. Cluster analysis

To evaluate temporal changes in zooplankton biovolume, a cluster analysis was performed. Biovolume data between 0.35 and 5.0 mm ESD, covering the size range of major zooplankton, were binned into 47 size classes at 0.1-mm ESD intervals. Biovolume data (X: mm^3 m^{-2}) were normalized as $\log_{10}(X+1)$. Similarities between zooplankton samples were then calculated using the Bray-Curtis similarity index. To group the samples, similarity indices were coupled with hierarchical agglomerative

138 clustering using a complete linkage method (Unweighted Pair Group Method using
139 Arithmetic Mean: UPGMA; Field et al., 1982). Non-metric multidimensional scaling
140 (NMDS) ordination was performed to distribute the sample groups on a
141 two-dimensional map (Field et al., 1982). To clarify which environmental parameters
142 (temperature, salinity, Chl. *a*, NO_3, rainfall, wind direction, or wind speed) exhibited
143 significant relationships with the zooplankton sample groups, multiple regression
144 analyses were performed using StatView (SAS Institute Inc.).

145 Before OPC measurement, zooplankton species were identified under a
146 stereomicroscope using 1/5 −1/20 aliquots of zooplankton samples. To evaluate the
147 zooplankton species characterizing each community group, inter-group differences in
148 abundance were tested for the top 20 most abundant zooplankton species by using
149 one-way ANOVA.

150 *2.4. Normalized Biomass Size Spectra*

151 Due to underestimation in the smallest size class (i.e., 300-400 μm), this class
152 was removed to calculate the fit model in NBSS analysis. From the OPC data,
153 zooplankton biovolumes (mm^3 m^{-3}) between 0.40 and 5.0 mm ESD were averaged for
154 each 0.1-mm ESD size class. To calculate the *X*–axis of the NBSS (*X*: $\log_{10}$

zooplankton biovolume [mm^3]), the biovolume of each size class (mm^3) was converted into a common logarithm. To calculate the *Y*–axis of the NBSS (*Y*: $\log_{10}$ zooplankton biovolume [mm^3 m^{-3}] / Δbiovolume [mm^3]), the biovolume was divided by the biovolume interval (Δbiovolume [mm^3]) and converted to a common logarithm. Based on these data, the NBSS linear model was calculated as follows:

$$Y = aX + b$$

where *a* and *b* are the slope and intercept of the NBSS, respectively.

2.5. Structural Equation Modelling analysis

SEM analysis was performed to evaluate the factors governing the changes in zooplankton abundance and biovolume, NBSS slope and NBSS intercept (Stomp et al., 2011). For SEM analysis, atmospheric parameters (rainfall, wind speed and wind direction), hydrographic parameters (daily differences in tide level, temperature, salinity, Chl. *a* and NO_3) and zooplankton parameters (abundance, biovolume, NBSS slope and intercept) were transformed into normalized values (average= 0, standard deviation= 1), and correlation coefficients between all parameters were calculated. For the path analysis, we sorted the parameters into the following three categories, 1: atmospheric parameters, 2: hydrographic parameters, and 3: zooplankton parameters.

3. Results

3.1. Hydrography

In 2011, sea ice was present from January 19 to March 4 at Mombetsu, and its retreat was approximately 20 days earlier than normal (1st Regional Coast Guard website). Throughout the study period, the integrated mean temperature ranged from -1.7 to 21.6°C; it was low during February and high from the end of August to September (Fig. 2a). The integrated mean salinity ranged from 30.6 to 33.7 and was low with little variability from the end of November to March, whereas it was high with great variability from April to October (Fig. 2a). The nutrient NO_3 ranged from 0.07 to 30.05 μM and was high during January. High nutrients occurred occasionally in June, which corresponded with times of low salinity (Fig. 2b). Chl. *a* ranged from 0.3 to 15.8 μg L^{-1}, showing high values from February to March (Fig. 2b). Daily differences in tidal level ranged from 30 to 138 cm with low variability in March and September (Fig. 2c). Air temperature ranged from -11.9 to 27.0˚C, and it was low and high in January and August, respectively (Fig. 2d). The daily amount of rainfall was high during the summer (Fig. 2d). High daily amounts of rainfall during July to October induced a sudden, concurrent decrease in salinity (<32). The daily maximum

189 wind speed ranged from 2.2 to 11.8 m s^{-1}, was dominated by a westerly wind and was
190 faster during the winter (Fig. 2e).

191 *3.2. OPC calibration*

192 For zooplankton abundance, a comparison between microscopic data (*X*) and
193 OPC data (*Y*) showed a highly significant correlation, and the values from the OPC
194 data were slightly lower (0.897 times) than those from the microscopic data (Y=0.897X,
195 r^2=0.856, p<0.0001, Fig. 3).

196 *3.3. Temporal changes*

197 The zooplankton abundance by OPC ranged from 2,206 to 203,158 ind. m^{-2}
198 and was high during April (Fig. 4a). The zooplankton abundance based on
199 microscopic observation ranged from 2,027 to 215,706 ind. m^{-2} and was also high
200 during April (Fig. 4b). The zooplankton biovolume based on OPC ranged from 386 to
201 30,685 mm^3 m^{-2} and was high from March to May and low from August to November
202 (Fig. 4a). The NBSS slope ranged from -2.37 to -0.628 and was lower than -1 from
203 June to December (Fig. 4b). Further, the NBSS intercept ranged from -0.629 to 1.265
204 and was high between late March to April and in early July (Fig. 4c).

205 *3.4. Cluster analysis based on zooplankton biovolume*

206 Based on the biovolume size spectra, zooplankton communities were classified
207 into six groups (A–F) at 40% dissimilarity by cluster analysis (Fig. 5a). Within the
208 hydrographic parameters, the integrated mean temperature had a significant relationship
209 with the NMDS of each group (Fig. 5b). Each group occurred separately by season.
210 Thus, group A was observed from January to February, group C occurred from March to
211 May, Group E was observed from March to April, group F was observed from April to
212 May, group B was observed from July to December, and group D was observed from
213 November to June (Fig. 4). According to Hamasaki et al. (1998), size-fractionated Chl.
214 *a* at Mombetsu Harbour was classified into three seasonal periods as follows: summer
215 (June-October), winter (November-February and April-May) and ice-covered (March).
216 For the zooplankton size spectra in this study, groups B and A were observed during
217 summer and winter, respectively, which correspond to the seasonal periods of Chl. *a*
218 (Fig. 4). However, the remaining groups C-F were observed from March to June and
219 showed short-term exchanges in that period, which indicates that frequent temporal
220 changes in zooplankton size spectra occurred in that period (Figs. 2, 4).

221 Except for group C, the zooplankton biovolume was dominated by the smaller

0.35 to 1-mm ESD size class (Fig. 5c). Few of the zooplankton in the large 4- to 5-mm ESD size class were in groups A and B, but they dominated group C. The zooplankton size spectra were similar for groups D and E, whereas the mean biovolume was approximately three times higher for group E than it was for group D. Zooplankton size was dominated by a larger size class in group F than in groups D and E.

3.5. Taxonomic accounts

Among the most numerous zooplankton (top 20 species in annual mean abundance) based on microscopic observation, euphausiids (*Euphausia pacifica* and *Thysanoessa inermis*), copepods (*Eurytemora herdmani*, *Acartia longiremis*, *Tortanus discaudatus*), brachyurans larvae, cladocerans (*Pleopis polyphemoides*, *Podon leuckarti*), hydrozoans, gastropods and echinopluteus larvae showed significantly different abundance between the zooplankton groups separated by OPC biovolume (Table 1). Group B was characterized by a dominance of cladocerans (*P. polyphemoides* and *P. leuckarti*) and echinopluteus larvae. Group C was dominated by euphausiids. Group D was dominated by the copepod *A. longiremis*, barnacle larvae and gastropods. Group E was dominated by the copepod *E. herdmani* and brachyurid

239 larvae. Group F was dominated by the copepod *T. discaudatus* and hydrozoans. No
240 species showed a high abundance in group A.

241 *3.6. NBSS in clustering group*

242 The mean NBSS of each group is shown in Fig. 6. The NBSS slope and
243 intercept for group A were both low. The steepest NBSS slope was seen for group B.
244 For groups A, D and E, prominent peaks were observed around -1 of the *X*-axis ($\log_{10}$
245 zooplankton biovolume [mm^3]), and a peak for group C was seen at approximately -1.5.
246 These peaks corresponded to the sizes of the abovementioned abundant species. Thus,
247 the peak of group B consisted of cladocerans; group C peaks corresponded to
248 euphausiid eggs and nauplii and the large copepod *Neocalanus cristatus* C5; the peak of
249 group D consisted of copepod *A. longiremis*; and the peak of group E was composed of
250 copepod *E. herdmani* (Fig. 6).

251 *3.7. SEM analysis*

252 From the SEM analysis, of the eight environmental parameters (rainfall, wind
253 speed, wind direction, daily differences in tidal level, water temperature, salinity, Chl. *a*,
254 and NO_3), high correlations were observed between temperature and salinity (path

255 coefficients: pc= 0.55-0.56) (Fig. 7). Regarding zooplankton parameters, zooplankton
256 abundance and biovolume had common negative correlations with temperature (pc
257 ranged from -0.50 to -0.65). The slope of the NBSS showed no relationship to any of
258 the parameters. The intercept had positive and negative correlations with rainfall and
259 NO_3, respectively.

260 *3.8. Seasonality of water mass with hydrography and zooplankton community*

261 In this study, the ranges of water temperature and salinity for each zooplankton
262 cohort were classified into three groups (Fig. 8). Group A had the lowest water
263 temperature and salinity, group B had the highest water temperature and salinity, and
264 groups C-F showed moderate water temperatures of approximately 3–7°C and a salinity
265 of 32–33 (Fig. 8). From the water mass classification in this area (Aota, 1975;
266 Takizawa, 1982), group A was classified into the East Sakhalin Current Water, groups
267 C-F were in the Okhotsk Surface Water and group B was considered a mixture of
268 Okhotsk Surface Water and Soya Warm Current Water. The warm and saline group B
269 was seen from July to December, and no other groups occurred during that time period
270 (Fig. 4).

4. Discussion

4.1. OPC measurement

The OPC has been used in numerous studies (Sprules et al., 1998; Nogueira et al., 2004; Zhou et al., 2009); however, some papers have reported on the weaknesses of the OPC measurement for the evaluation of zooplankton communities. First, OPC cannot detect whether the particles are organisms or non-organisms (e.g., detritus, fragments of copepods). For this reason, multiple measurements by OPC tend to overestimate the abundance in the fixed samples due to fragmentation (Sprules et al., 1998; Beaulieu et al., 1999; Zhang et al., 2000). Additionally, since the device measures the size of particles based on the extent of attenuation of a light beam, coincident counts (i.e., two or more particles coincident in the light beam, resulting in a single count and a size measurement equal to the sum of the particles), particle shapes (e.g., slenderness) and the degree of particle transparency could cause underestimates of both the biovolume and particle numbers (Herman, 1992; Sprules et al., 1998; Zhang et al., 2000). In this study, our measurement methods followed those of Yokoi et al. (2008), as mentioned as above. Furthermore, size classes smaller than the mesh size of the net (335 μm) were removed because smaller size classes could be non-quantitative and/or underestimated. These conditions and pretreatments of the data set could

289 indicate a good relationship between the microscopic count and the OPC measurement.

290 *4.2. Temporal changes*

291 Both zooplankton abundance and biovolume showed a negative correlation
292 with water temperature in SEM analysis (Fig. 7). The ranges of water temperature and
293 salinity were different among the zooplankton groups (Fig. 8). The zooplankton
294 community in the southern Okhotsk Sea is known to vary between cold-water and
295 warm-water species; i.e., cold-water species occur at <12°C and <33.6 salinity, whereas
296 warm-water species occur at >12°C and >33.6 salinity (Asami et al., 2007).
297 Cold-water species include the copepods *N. cristatus*, *Pseudocalanus minutus*, *P.*
298 *newmani*, *Metridia pacifica* and *M. okhotensis* (Asami et al., 2009; Shimada et al.,
299 2012). These cold-water species are also known to be dominant in basin areas of the
300 Okhotsk Sea (Itoh et al., 2014). As warm-water species, the following three copepods
301 were abundant: *Paracalanus parvus* s.l., *Acartia steueri* and *A. hudsonica* (Asami et al.,
302 2007).

303 During the ice-covered period, zooplankton may feed mainly on ice algae
304 (Hiwatari et al., 2008). Once the ice has melted, an ice edge bloom is initiated
305 (Mustapha and Saitoh, 2008). After the ice retreats, the water mass at the surface layer

306 is characterized by the less saline Okhotsk Surface Water (Aota, 1975). The volume
307 transport of the Soya Warm Current is lowest during winter, increasing from May to
308 June, and reaches a maximum in autumn (Takizawa, 1982). The volume transport of
309 the counterpart cold East Sakhalin Current is known to be greater during winter
310 (Oshima et al., 2002). The variability of the volume transport of the Soya Warm
311 Current and the East Sakhalin Current corresponds well to the differences in water
312 levels between the Japan Sea and Okhotsk Sea (Aota, 1975).

313 From summer (July) to winter (November), the zooplankton community
314 consisted of one group (Group B). This corresponds to the period of intensive flow of
315 the Soya Warm Current (Aota, 1975). As shown in the T-S diagrams of the Mombetsu
316 Harbour, the water was sufficiently warm but had lower saline content during this
317 season (Fig. 8). This lower saline water is considered to be modified Soya Warm
318 Current Water, and because the present study area is located in a coastal area, the
319 addition of fresh water such as rainfall and river runoff (see spikes in Fig. 2d) induced
320 decreases in salinity (Fig. 2a). There seemed to be a link between rainfall and low
321 salinity (Fig. 2), but the effect on zooplankton of these parameters was unclear because
322 rainfall and NO_3 showed a positive and negative effect on zooplankton biovolume and
323 intercept; further, there was no relationship with salinity according to the SEM analysis.

Thus, prominent characteristics of seasonality in zooplankton at Mombetsu Harbour include stability and less variability at low zooplankton biovolumes, and size spectra and community structure similarities were observed from summer to winter when covered by modified Soya Warm Current Water.

4.3. Taxonomic accounts

Species composition can help improve our understanding of the seasonality and distribution of the zooplankton community size spectra at Mombetsu Harbour. *P. polyphemoides*, which is dominant in group B, is known to be abundant in neritic and estuarine environments (Bosch and Taylor, 1973; Onbé, 1974). *P. leuckarti* and *E. nordmanni* are classified as cold-water species in Toyama bay (Onbé and Ikeda, 1995). These cladocerans are known to have resting eggs (Onbé, 1978). The hatching of resting eggs of *E. nordmanni* is reported to be possible at temperatures of 5-20°C (Komazawa and Endo, 2002). In Mombetsu Harbour, low temperatures (<5°C) were seen from December to May (Fig. 2a). Cladocerans generally spend that cold season as resting eggs in the bottom mud.

In group C, euphausiid eggs, nauplii and the large copepod *N. cristatus* were found to be important species based on the results of one-way ANOVA and NBSS.

341 Offshore in the southern Okhotsk Sea, *N. cristatus* was dominated by C1-C3 stages
342 during spring and was composed of C4-C5 stages from summer to autumn (Tsuda et al.,
343 2015). In this study, *N. cristatus* C5 occurred in group C during spring. This
344 occurrence would be partly caused by the high Chl. *a* of the neritic zone found in this
345 study during March (>5 μg L^{-1}, Fig. 2b). The high Chl. *a* in Mombetsu Harbour may
346 accelerate the development of *N. cristatus*. Thus, dominance of the C5 stages of *N.*
347 *cristatus* may be observed with a much faster timing than in the offshore region. The
348 dominance of euphausiid eggs and nauplii may also be a reflection of this large spring
349 phytoplankton bloom. Therefore, the reproduction of euphausiids may be achieved by
350 the spring phytoplankton bloom from February to March, and their resulting eggs and
351 nauplii may dominate group C from March to April (Table 1).

352 From January to February, the zooplankton community was represented by
353 only group A and had the lowest biovolume. Because the time period of January to
354 February was characterized by sea ice coverage and had the coldest temperatures (Fig.
355 2a), a low hatchability of resting eggs and slow zooplankton growth may have led to the
356 low zooplankton biovolume that was observed during that time.

357 Seasonal occurrence timing varied for the abovementioned zooplankton groups
358 (A, B and C), while the remaining groups (D, E and F) occurred in overlapping seasons.

In particular, from April to May, four zooplankton groups (C, D, E and F) were found, and the zooplankton size spectra showed high short-term variability (Fig. 4). The plotted areas of the four groups overlapped in the T-S diagrams, and classification was difficult when using physical oceanography (Fig. 8) parameters. However, the zooplankton biovolume and size spectra showed great differences between groups (Fig. 5c). Thus, it was possible to classify each group from the viewpoint of biological oceanography. The dominant species varied among groups D, E and F (Table 1). For copepods, groups D, E, and F were characterized by a greater abundance of *A. longiremis*, *E. herdmani* and *T. discaudatus*, respectively. Among them, *A. longiremis* and *T. discaudatus* are known to have resting eggs in the bottom sediment (Marcus, 1990; Marcus et al., 1994). Although no information is available on the resting eggs of *E. herdmani*, the congener *E. affinis* is reported to have resting eggs (Marcus et al., 1994) and has a high abundance around the ice edge (Coyle and Cooney, 1988). Thus, from the viewpoints of the hatching of resting eggs, the ice edge and the spring phytoplankton bloom, the spatial and temporal heterogeneity in the biological environment is expected to be high from April to May. This phenomenon provides greater temporal variability in zooplankton communities within a short time period.

376 *4.4. NBSS characteristics*

377 NBSS is derived from zooplankton biomass size spectra and is known to be an
378 index of productivity of marine ecosystems, transfer efficiency to higher trophic levels
379 and predator-prey interactions (Herman and Harvey, 2006; Zhou, 2006). The NBSS
380 slope is known to vary with biomass productivity, energy transfer efficiency and
381 predator-prey interactions (Zhou, 2006; Zhou et al., 2009). Under a theoretical steady
382 state, the slope settles around -1, while slopes steeper than -1 indicate high productivity
383 but low energy transfer efficiency, and slopes flatter than -1 indicate low productivity
384 but high energy transfer efficiency (Sprules and Munawar, 1986). According to
385 Vandromme et al. (2014), a slope flatter than -1 indicates post-bloom conditions
386 because larger zooplankton species are observed later in the productive season (e.g.,
387 spring) than smaller ones are. Additionally, steeper NBSS slopes indicate high
388 productivity due to the higher proportion of herbivorous zooplankton (Zhou et al., 2009).
389 If steeper slopes are found in oligotrophic situations, it means that the slopes are
390 supported by primary production of microbial food webs (Iriarte and González, 2004).

391 In the present study, the NBSS slope varied among the groups, ranging from –
392 0.85 (group C) to –1.52 (group B). Groups A and C showed flatter slopes (–0.85 - –
393 1.1) than the other groups (–1.31 - –1.52) (Fig. 6). These groups were observed in

394 cold and less saline conditions (Fig. 8) from January to April (Fig. 4). On the other
395 hand, slopes steeper than -1 were the case for groups B, D, E and F. Among them, the
396 slope of group B from summer to winter was the steepest (-1.52) for the zooplankton
397 communities at Mombetsu Harbour. Overall, the slopes of zooplankton NBSS in
398 Mombetsu Harbour showed the following clear seasonal patterns: they were flatter from
399 winter to spring and steeper from summer to autumn. These seasonal patterns
400 corresponded well to the water mass exchanges. For the winter-spring East Sakhalin
401 Current, low productivity under cold conditions would occur, with high transfer
402 efficiency to large-sized plankton. In contrast, in the summer-autumn Soya Warm
403 Current, high productivity would occur under warm and stable conditions, with a low
404 transfer efficiency and few large-sized plankton expected.

405 The NBSS slopes based on zooplankton biovolume (the same unit in this
406 study) from worldwide oceans are summarized in Table 2. In several studies, seasonal
407 or spatial changes in NBSS slopes within the region were reported. For instance, the
408 NBSS slopes for offshore regions and estuaries in the Gulf of St. Lawrence were
409 reported to be -0.47 and -0.90, respectively (Herman and Harvey, 2006). For the
410 Brazilian Continental Shelf, the NBSS slopes for offshore and neritic regions were
411 reported to be -0.86 and -1.25, respectively (Marcolin et al., 2013). For the Chukchi

412 Sea, the NBSS slopes for oligotrophic and eutrophic regions were -0.86 and -1.11,
413 respectively (Matsuno et al., 2012). For the western Antarctic Peninsula, the NBSS
414 slopes during autumn and summer are reported to be -0.92 and -1.80, respectively
415 (Zhou et al., 2009). Thus, these studies show that NBSS slopes were steeper for the
416 high productivity season/region. The variation of NBSS slopes within a region (ratio
417 between maximum: minimum in NBSS slopes) was calculated to range from 1.29 to
418 1.96 (mean±sd: 1.65±0.33) (Table 2).

419 In the present study, the NBSS slopes at Mombetsu Harbour ranged from -0.85
420 to -1.52, and the variation in NBSS slope (maximum: minimum) was 1.79. This value
421 was within the variations observed for the abovementioned regions. The NBSS slopes
422 were within the reported values of between -0.47 offshore of the Gulf of St. Lawrence
423 (Herman and Harvey, 2006) and -2.30 in the California Bay (Napp et al., 1993) (cf.
424 Table 2). These facts suggest that, while seasonal variability was great, the NBSS of
425 zooplankton communities at Mombetsu Harbour are typical. The occurrence
426 frequency of highly productive groups (groups A, B, D, E and F) was 95.2%
427 (=100/105*100), and they were defined by steeper slopes, indicating a high productivity
428 of zooplankton (Zhou et al., 2009). This finding indicates that the zooplankton
429 community structure changes seasonally with water mass exchanges, but the

productivity was continuously high at Mombetsu Harbour throughout the year.

4.5. Conclusion

The hydrography of Mombetsu Harbour is characterized by temporal ice coverage in winter and the exchange of the following two water masses: the Soya Warm Current and the East Sakhalin Current. Zooplankton size spectra were within the ranges similar to those of previous reports and were divided into three seasonal regimes.

During the ice-covered period (January to February), zooplankton abundance was low because of the low productivity and lower levels of resting egg hatching under cold conditions. During the ice-retreat from March to May, an ice-edge bloom formed, reproduction of euphausiids occurred, and zooplankton biomass was high. During spring, although the physical parameters (e.g., water temperature and salinity) were similar, several zooplankton communities, as characterized by different size spectra and taxonomic accounts, were exchanged over a short period. These facts suggest that the spatio-temporal variability in zooplankton communities was the most prominent during that season. From summer to winter (June to December), the Soya Warm Current was present, zooplankton biomass was low and steady, and cladocerans dominated, which may have been due to the hatching of resting eggs.

From the SEM analysis, zooplankton abundance and biovolume showed negative correlations with water temperature. This relationship was a reflection of the water mass exchanges that are characterized by greater differences in water temperature. Although there was a clear seasonality in the zooplankton community and size spectra, the frequency of highly productive groups occurred at a high level (95.2%) throughout the year. This indicates that the zooplankton community structure changed seasonally with water mass exchanges but that the productivity was kept continuously high in almost all periods during the year at Mombetsu Harbour.

Acknowledgements

We thank Prof. Ichiro Imai for providing valuable comments on an earlier version of the manuscript. Part of this study was supported by a Grant–in–Aid for Scientific Research 17H01483 (A), 16H02947 (B) and 15KK0268 (Joint International Research) from the Japanese Society for Promotion of Science (JSPS). This work was partially conducted for the Arctic Challenge for Sustainability (ArCS) project.

References

Aota, M., 1975. Studies on the Soya Warm Current. Low. Temp. Sci., (Ser. A), 33, 151−172 (in Japanease).

Asami, H., Shimada, H., Sawada, M., Sato, H., Miyakoshi, Y., Ando, D., Fujiwara, M. and Nagata, M., 2007. Influence of physical parameters on zooplankton variability during early ocean life of juvenile chum salmon in the coastal waters of eastern Hokkaido, Okhotsk Sea. N. Pac. Anadr. Fish Comm. Bull. 4, 211–221.

Asami, H., Shimada, H., Sawada, M., Miyakoshi, Y., Ando, D., Fujiwara, M. and Nagata, M., 2009. Spatial and seasonal distributions of copepods from spring to summer in the Okhotsk Sea off eastern Hokkaido, Japan. PICES Sci. Rep., 36, 233−239.

Basedow, S.L., Tande, K.S. and Zhou, M., 2010. Biovolume spectrum theories applied: spatial patterns of trophic levels within a mesozooplankton community at the polar front. J. Plankton Res., 32, 325−349.

Beaulieu, S.E., Mullin, M.M., Tang, V.T., Pyne, S.M., King, A.L. and Twining, B.S., 1999. Using an optical plankton counter to determine the size distributions of preserved zooplankton samples. J. Plankton Res., 21, 1939−1956.

480 Bosch, H.F. and Taylor, W.R., 1973. Distribution of the cladoceran *Podon*
481 *polyphemoides* in the Chesapeake Bay. Mar. Biol., 19, 161–171.
482 Coyle, K.O. and Cooney, R.T., 1988. Estimating carbon flux to pelagic grazers in the
483 ice−edge zone of the eastern Bering Sea. Mar. Biol., 98, 229−306.
484 Ducklow, H.W., Steinberg, D.K. and Buesseler, K.O., 2001. Upper ocean carbon export
485 and the biological pump. Oceanography, 14, 50−58.
486 Field, J.G., Clarke, K.R. and Warwick, R.M., 1982. A practical strategy for analysing
487 multispecies distribution patterns. Mar. Ecol. Prog. Ser., 8, 37−52.
488 Fukamachi, Y., Tanaka, I., Oshima, I., Ebuchi, N., Mizuta, G., Yoshida, H., Takayanagi,
489 S. and Wakatsuchi, M., 2008. Volume transport of the Soya Warm Current
490 revealed by Bottom–Mounted ADCP and Ocean–Radar measurement. J.
491 Oceanogr., 64, 385–392.
492 Hamasaki, K., Ikeda, M., Ishikawa, M., Shirasawa, K. and Taguchi, S., 1998. Seasonal
493 variability of size–fractionated chlorophyll a in Monbetsu Harbor, Hokkaido,
494 northern Japan. Plankton Biol. Ecol., 45, 151–158.
495 Herman, A. W., 1988. Simultaneous measurement of zooplankton and light attenuance
496 with a new optical plankton counter. Cont. Shelf Res., 8, 205−221.
497 Herman, A. W., 1992. Design and calibration of a new optical plankton counter capable

498 of sizing small zooplankton. Deep-Sea Res., 39, 395−415.
499 Herman, A. W. and Harvey, M., 2006. Application of normalized biomass size spectra to
500 laser optical plankton counter net intercomparisons of zooplankton
501 distributions J. Geophys. Res., 111, C05S05.
502 Hiwatari, T., Shirasawa, K., Fukamachi, Y., Nagata, R., Koizumi, T., Koshikawa, H. and
503 Kohata, K., 2008. Vertical material flux under seasonal sea ice in the Okhotsk
504 Sea north of Hokkaido, Japan. Polar Sci. 2, 41–54
505 Iriarte, J.L. and González, H.E., 2004. Phytoplankton size structure during and after the
506 1997/98 El Nino in a coastal upwelling area of the northern Humboldt
507 Current System. Mar. Ecol. Prog. Ser., 269, 83−90.
508 Itoh, H., Nishioka, J. and Tsuda, A., 2014. Community structure of mesozooplankton in
509 the western part of the Sea of Okhotsk in summer. Prog. Oceanogr., 126, 224–
510 232.
511 Kasai, H., Nagata, R., Murai, K., Katakura, S., Tateyama, K. and Hamaoka, S., 2017.
512 Seasonal change in oceanographic environments and the influence of
513 interannual variation in the timing of sea-ice retreat on Chlorophyll a
514 concentration in the coastal water of northeastern Hokkaido along the
515 Okhotsk Sea. Bull. Coast. Oceanogr., 54, 181−192.

516 Komazawa, H. and Endo, Y., 2002. Experimental studies on hatching conditions of the
517 resting eggs of marine Cladocerans and their seasonal variation in Onagawa
518 Bay. Tohoku J. Agric. Res., 52, 57–85.
519 Marcolin, C.R., Schultes, S., Jackson, G.A. and Lopes R.M., 2013. Plankton and seston
520 size spectra estimated by the LOPC and ZooScan in the Abrolhos Bank
521 ecosystem (SE Atlantic). Cont. Shelf Res., 70, 74−87.
522 Marcus, N.H., 1990. Calanoid copepod, cladoceran, and rotifer eggs in sea−bottom
523 sediments of northern California coastal waters: identification, occurrence
524 and hatching. Mar. Biol., 105, 413−418.
525 Marcus, N.H., Lutz, R., Burnett, W. and Cable, P., 1994. Age, viability, and vertical
526 distribution of zooplankton resting eggs from an anoxic basin: Evidence of an
527 egg bank. Limnol. Oceanogr., 39, 154−158.
528 Matsuno, K., Yamaguchi, A. and Imai, I., 2012. Biomass size spectra of
529 mesozooplankton in the Chukchi Sea during the summers of 1991/1992 and
530 2007/2008: an analysis using optical plankton counter data. J. Mar. Sci., 69,
531 1205–1217.
532 van der Meeren, T. and Næss, T., 1993. How does cod (*Gadus morhua*) cope with
533 variability in feeding conditions during early larval stage? Mar. Biol., 116,

637−647.

Michaels, A.F. and Silver, M.W., 1988. Primary production, sinking fluxes and microbial food web. Deep‑Sea Res., 35A, 473−490.

Moore, S.K. and Suthers, I.M., 2006. Evaluation and correction of subresolved particles by the optical plankton counter in three Australian estuaries with pristine to highly modified catchments. J. Geophys. Res., 111, C05S04.

Mustapha, M.A. and Saitoh, S., 2008. Observations of sea ice interannual variations and spring bloom occurrences at the Japanese scallop farming area in the Okhotsk Sea using satellite imageries. Estuar. Coast. Shelf Sci., 77, 577–588.

Napp, J.M., Ortner, P.B., Pieper, R.E. and Holliday, D.V., 1993. Biovolume–size spectra of epipelagic zooplankton using a Multi–frequency Acoustic Profiling System (MAPS). Deep–Sea Res. I, 40, 445−459.

Nogueira, E., González-Nuevo, G., Bode, A., Varela, M., Anxelu, X., Morán, A.G. and Valdés, L., 2004. Comparison of biomass and size spectra derived from optical plankton counter data and net samples: application to the Northwest and North Iberian Shelf. J. Mar. Sci., 61, 508−517.

Onbé, T., 1974. Studies on the ecology of marine cladocerans. J. Fac. Fish. Anim. Husb., Hiroshima Univ., 13, 83–179 (In Japanese with English abstract).

552 Onbé, T., 1978. The life cycle of marine cladocerans. Bull. Plankton Soc. Japan, 25,
553 41−54 (In Japanese with English abstract).
554 Onbé, T. and Ikeda, T., 1995. Marine cladocerans in Toyama Bay, southern Japan Sea:
555 seasonal occurrence and day–night vertical distributions. J. Plankton Res., 17,
556 595–609.
557 Oshima, K. I., Wakatsuchi, M. and Fukamachi, Y., 2002. Near–surface circulation and
558 tidal currents of the Okhotsk Sea observed with satellite–tracked drifters. J.
559 Geophys. Res., 107(C11), 3195.
560 Sato, K., Matsuno, K., Arima, D., Abe, Y. and Yamaguchi, A., 2015. Spatial and
561 temporal changes in zooplankton abundance, biovolume, and size spectra in
562 the neighboring waters of Japan: analyses using an optical plankton counter.
563 Zool. Stud., 54, 1–15.
564 Shimada, H., Sakaguchi, K., Mori, Y., Watanobe, M., Itaya, K. and Asamim, H., 2012.
565 Seasonal and annual changes in zooplankton biomass and species structure in
566 four areas around Hokkaido (Doto and Donan areas of the North Pacific, the
567 northern Japan Sea and the southern Okhotsk Sea). Bull. Plankton Soc. Japan,
568 59, 63–81.
569 Sprules, W.G. and Manuwar, M., 1986. Plankton size spectra in relation to ecosystem

productivity, size, and perturbation. Can. J. Fish. Aquat. Sci., 43, 1789−1986

Sprules, W.G., Herman, A.W. and Stockwell, J.D., 1998. Calibration of an optical plankton counter for use in fresh water. Limnol. Oceanogr., 43, 726−733.

Stomp, M., Huisman, J., Mittelbach, G.G., Litchman, E. and Klausmeier. C.A., 2011. Large-scale biodiversity patterns in freshwater phytoplankton. Ecology, 92, 2096−2107.

Takizawa, T., 1982. Characteristics of the Soya Warm Current in the Okhotsk Sea. J. Oceanogr. Soc. Japan, 38, 281–292

Tsuda, A., Saito, H., Kasai, H., Nishioka, J. and Nakatsuka, T., 2015. Vertical segregation and population structure of ontogenetically migrating copepods *Neocalanus cristatus*, *N. flemingeri*, *N. plumchrus*, and *Eucalanus bungii* during the ice–free season in the Sea of Okhotsk. J. Oceanogr., 71, 271–285.

Vandromme, P., Nogueira, E., Huret, M., Lopez-Urrutia, Á., González, G.G., Sourisseau, M. and Petitgas, P., 2014. Springtime zooplankton size structure over the continental shelf of the Bay of Biscay. Ocean. Sci., 10, 8321−835.

Yokoi, Y., Yamaguchi, A. and Ikeda, T., 2008. Regional and interannual changes in the abundance, biomass and community structure of mesozooplankton in the western North Pacific in early summer; as analyzed with an optical plankton

588 counter. Bull. Plankton Soc. Japan, 55, 79−88 (in Japanese with English
589 abstract).
590 Zhang, X., Roman, M., Sanford, A., Adolf, H., Lascara, C. and Burgett, R., et al., 2000.
591 Can an optical plankton counter produce reasonable estimates of zooplankton
592 abundance and biovolume in water with high detritus? J. Plankton. Res., 22,
593 137−150.
594 Zhou, M., 2006. What determines the slope of a plankton biomass spectrum? J.
595 Plankton Res., 28, 437−448.
596 Zhou, M., Tande, K.S., Zhu, Y. and Basedow, S., 2009. Productivity, trophic levels and
597 size spectra of zooplankton in northern Norwegian shelf regions. Deep–Sea
598 Res. II, 56, 1934–1944.
599

600 **Figure captions**

601 **Fig. 1.** (a) Location of Mombetsu, northeastern Hokkaido. Arrows indicate the
602 approximate direction of current flows. (b) Location of sampling station
603 (solid star, depth ca. 9 m) at Mombetsu harbor.

604 **Fig. 2.** Seasonal changes in environmental parameters. (a) Daily mean sea water
605 temperature and salinity in 0–9 m water column, (b) chlorophyll *a* and nutrients
606 (NO_3) at sea surface, (c) daily differences in tidal level, (d) air temperature and
607 daily amount of rainfall, (e) maximum wind speed and direction at Mombetsu
608 from January to December 2011. The sea ice observation period is shown by
609 a horizontal bar at the top abscissa.

610 **Fig. 3.** Relationship between zooplankton abundance values derived from OPC counts
611 and microscopic counts. All samples collected at Mombetsu harbor from
612 January to December 2011 were included in this plot. The dashed line
613 indicates the position of 1:1.

614 **Fig. 4.** Seasonal changes in (a) zooplankton abundance and biovolume derived from
615 OPC measurement and (b) NBSS slope and (c) NBSS intercept based at
616 Mombetsu harbor from January to December 2011. Seasonal occurrence
617 periods of zooplankton groups (A–F), as identified by Bray–Curtis similarity

based on their community size distributions (cf. Fig. 5) are shown with upper bars. Values in the parentheses indicate the number of dates included in each group.

Fig. 5. (a) Results of cluster analysis based on mesozooplankton biovolume size spectra at Mombetsu harbor during 2011. Six groups (A–F) were identified at 40% Bray–Curtis similarity connected with UPGMA. Numbers in the parentheses indicate the number of dates each group contained. (b) NMDS plots of each group. The arrow and percentage indicate the direction of environmental parameters and the coefficient of determination (r^2), respectively. T: temperature. (c) Mean biovolume and size composition (ESD, mm) of each group.

Fig. 6. Mean NBSS of six groups (A–F) identified from cluster analysis based on mesozooplankton biovolume size spectra at Mombetsu harbor from January to December 2011 (cf. Fig. 5). Numbers in the parentheses indicate the number of samples belonging to each group. For the dominant zooplankton species in each group (cf. Table 1), the mean (symbols) and standard deviation (bars) of the biovolume data are shown in the panel.

Fig. 7. Results of structural equation model (SEM) analysis for total zooplankton (a)

abundance and (b) biovolume and NBSS (c) slope and (d) intercept. The values along the pathways represent standardized path coefficients. Arrows with solid or dashed lines indicate positive or negative effects. The thickness of the arrows varies with the path coefficient values. The overall fit of the model was evaluated using the goodness–of–fit index (GFI) and the adjunct goodness–of–fit index (AGFI). Tide: daily differences of tidal level, Tem: sea temperature, Sal: salinity, Rainfall: daily amount of rainfall, Wind speed: daily maximum wind speed, Wind degree: daily maximum wind degree.

Fig. 8. T– S diagram of each zooplankton group. Symbols and bars indicate means and standard deviations, respectively. Water mass classifications by Takizawa (1982) are shown in the panel. S: Soya Warm Water, S': Forerunner of Soya Warm Water, IC: Intermediate Cold Water, O: Okhotsk Surface Water, E: East Sakhalin Current Water.

Table 1. List of zooplankton species occurring at Mombetsu harbor from Januray to December 2011. The top 20 species in annual mean abundance are only shown in this table. The abundance of each group (A-F) identified with zooplankton biovolumes is shown (cf. Fig. 5). Inter-group differences in abundance were tested by one-way ANOVA. For species showing significant differences between groups, the abundance of the highest group underlined.
*: $p<0.05$, **: $p<0.01$, ***: $p<0.001$, ****: $p<0.0001$, ns: not significant.

		Abundance (ind. m^{-3})							one-way
Taxa	lower taxa / Species	Annual mean	A	B	C	D	E	F	ANOVA
Euphausiids	Euphausiid egg and nauplii	7,631	0	8	36,475	29	3,889	31,488	***
Copepods	*Pseudocalanus newmani*	5,894	2,019	3,127	4,133	9,682	11,974	6,058	ns
Copepods	*Eurytemora herdmani*	5,359	2,674	76	8,277	5,608	52,883	4,231	****
Copepods	*Acartia longiremis*	3,167	1,484	161	1,646	8,866	7,235	959	****
Copepods	*Oithona atlantica*	1,549	109	1,481	762	2,051	1,620	1,430	ns
Cladocerans	*Evadne nordmanni*	1,218	0	2,309	0	297	1,705	606	ns
Appendicularians	*Fritillaria borealis*	1,045	87	807	347	1,604	103	1,368	ns
Decapods	Brachyura	1,028	0	527	4	1,162	7,024	866	*
Appendicularians	*Oikopleura longicauda*	919	0	807	0	2,073	157	47	ns
Barnacles	Balanomorpha	914	31	361	629	1,926	1,214	805	**
Echinoderms	Ophiopluteus larvae	877	0	2,128	8	1	0	31	ns
Copepods	*Tortanus discaudatus*	873	31	320	271	1,188	999	1,950	***
Cladocerans	*Pleopis polyphemoides*	835	0	1,981	0	0	22	130	****
Copepods	*Acartia hudsonica & omorii*	475	20	379	4	1,027	75	175	ns
Hydrozoans	*Rathkea* sp.	460	0	8	1,219	63	22	2,106	**
Gastropods	Gastropoda	428	0	183	116	1,037	90	312	*
Annelids	Polychaeta larvae	417	20	413	853	474	367	324	ns
Copepods	*Clausocalanus pergens*	293	0	375	19	266	112	330	ns
Echinoderms	Echinopluteus larvae	276	0	591	0	101	45	25	***
Cladocerans	*Podon leuckarti*	248	0	539	20	5	47	126	*
Others		2,957	725	3,531	2,634	2,504	2,662	4,382	ns

Table 2. Comparison of slope (a) of NBSS ($Y = aX + b$) based on mesozooplankton biovolume at various locations.

Location	Size range (mm)	Slope	References
Gulf of St Lawrence (open water)	0.25-2	-0.47	Herman and Harvey (2006)
Barents Sea	0.25-14	-0.63	Basedow et al. (2010)
Tasman Sea	0.11-3.3	-0.69	Baird et al. (2008)
Mombetsu (group C)	0.25-5	-0.85	This study
Brazilian Continental Shelf (Oceanic)	0.1-5	-0.86	Marcolin et al. (2013)
Chukchi Sea (less productive)	0.25-5	-0.86	Matsuno et al. (2012)
Gulf of St Lawrence (estuary)	0.25-2	-0.90	Herman and Harvey (2006)
Western Antarctic Peninsula (fall)	0.25-14	-0.92	Zhou et al. (2009)
NW Pacific	0.25-5	-0.93	Sato et al. (2015)
Coral Sea	0.11-3.3	-1.00	Suthers et al. (2006)
Mombetsu (group A)	0.4-5	-1.1	This study
Chukchi Sea (more productive)	0.25-5	-1.11	Matsuno et al. (2012)
Brazilian continental shelf (coastal)	0.1-5	-1.25	Marcolin et al. (2013)
Mombetsu (group E)	0.4-5	-1.36	This study
Mombetsu (group F)	0.4-5	-1.31	This study
Mombetsu (group D)	0.4-5	-1.37	This study
Mombetsu (group B)	0.4-5	-1.52	This study
Western Antarctic Peninsula (summer)	0.25-14	-1.80	Zhou et al. (2009)
California Bight	0.25-5	-2.30	Napp et al. (1993)

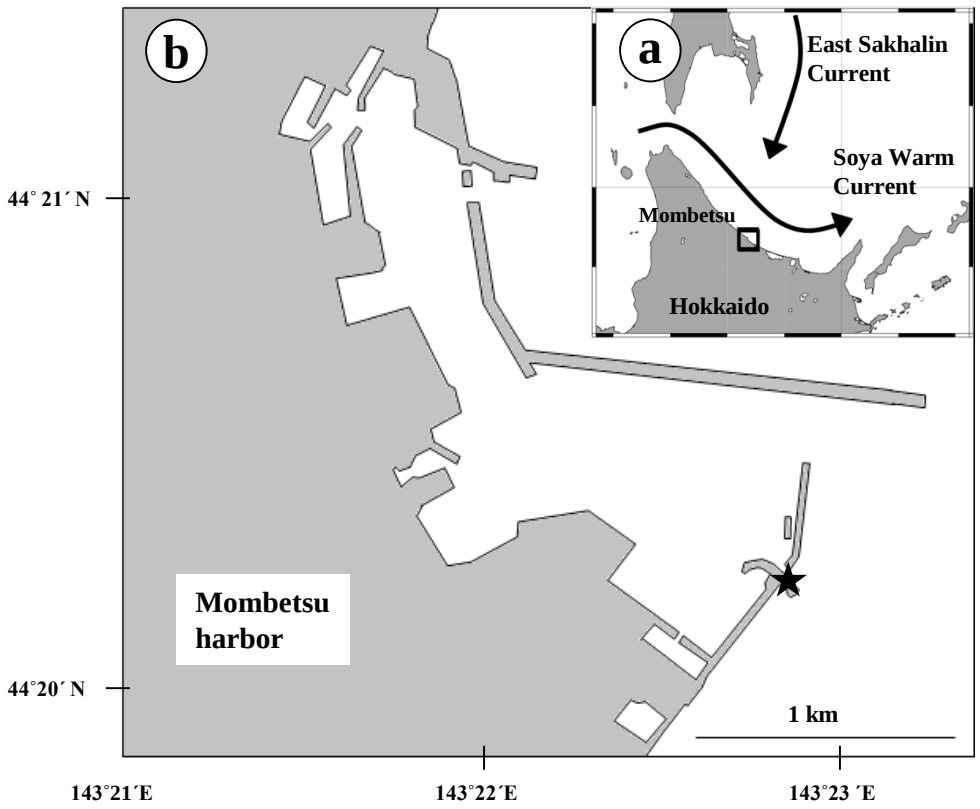

Fig. 1. (a) Location of Mombetsu, northeastern Hokkaido. Arrows indicate the approximate direction of current flows. (b) Location of sampling station (solid star, depth ca. 9 m) at Mombetsu harbor.

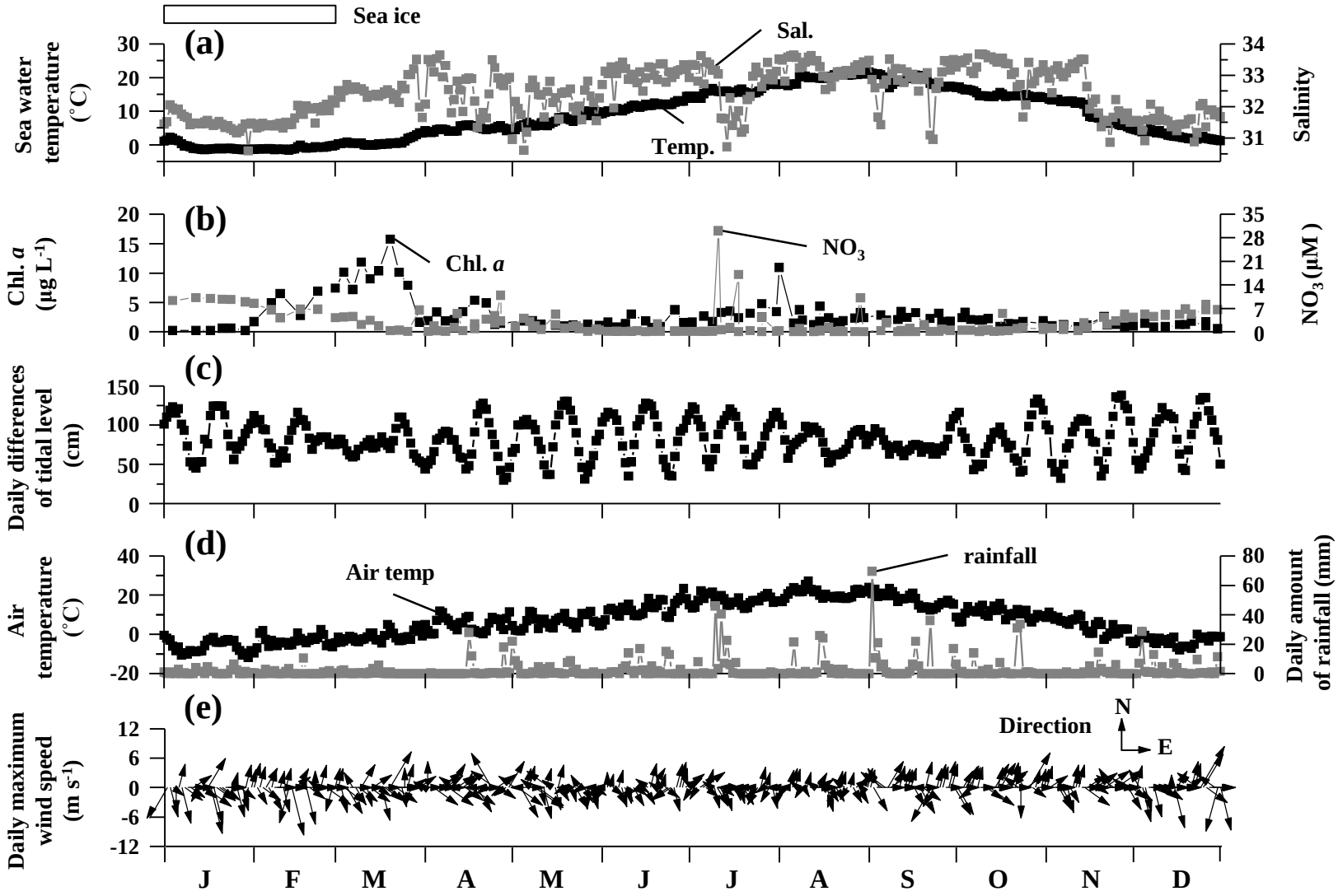

Fig. 2. Seasonal changes in environmental parameters. (a) Daily mean sea water temperature and salinity in 0-9 m water column, (b) chlorophyll *a* and nutrients (NO_3) at sea surface, (c) daily differences in tidal level, (d) air temperature and daily amount of rainfall, (e) maximum wind speed and direction at Mombetsu from January to December 2011. The sea ice observation period is shown by a horizonal bar at the top abscissa.

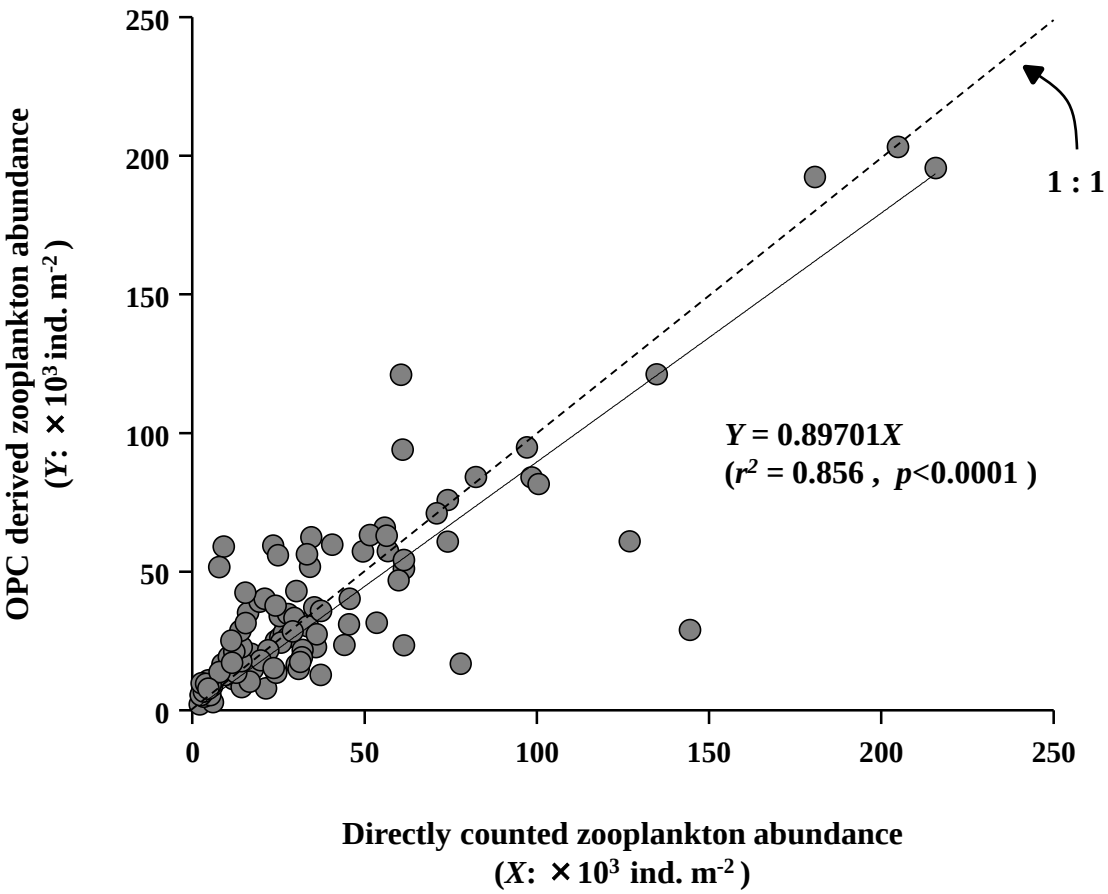

Fig. 3. Relationship between zooplankton abundances values derived from OPC counts and direct counts. All samples, collected at Mombetsu harbor from January to December 2011, were included in this plot. The dashed line indicates the position of 1:1.

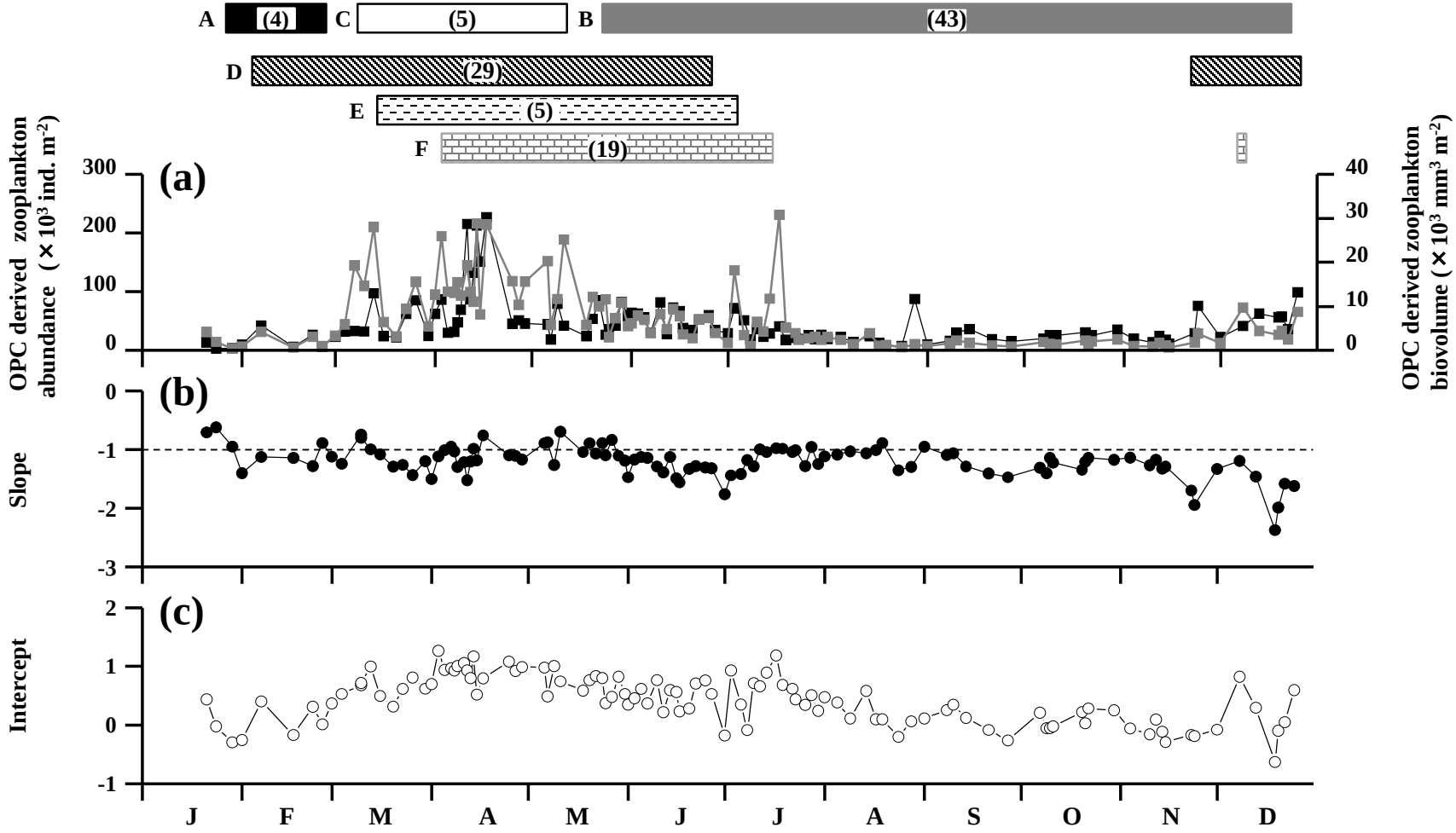

Fig. 4. Seasonal changes in (a) zooplankton abundance, biovolume, (b) NBSS slope and (c) NBSS intercept derived from OPC measurement at Mombetsu harbor from January to December 2011. Seasonal observed periods of zooplankton groups (A-F), as identified by Bray-Curtis similarity based on their community size distributions (cf. Fig. 5) are shown with upper bars. Values in the parentheses indicate the number of dates included in each group.

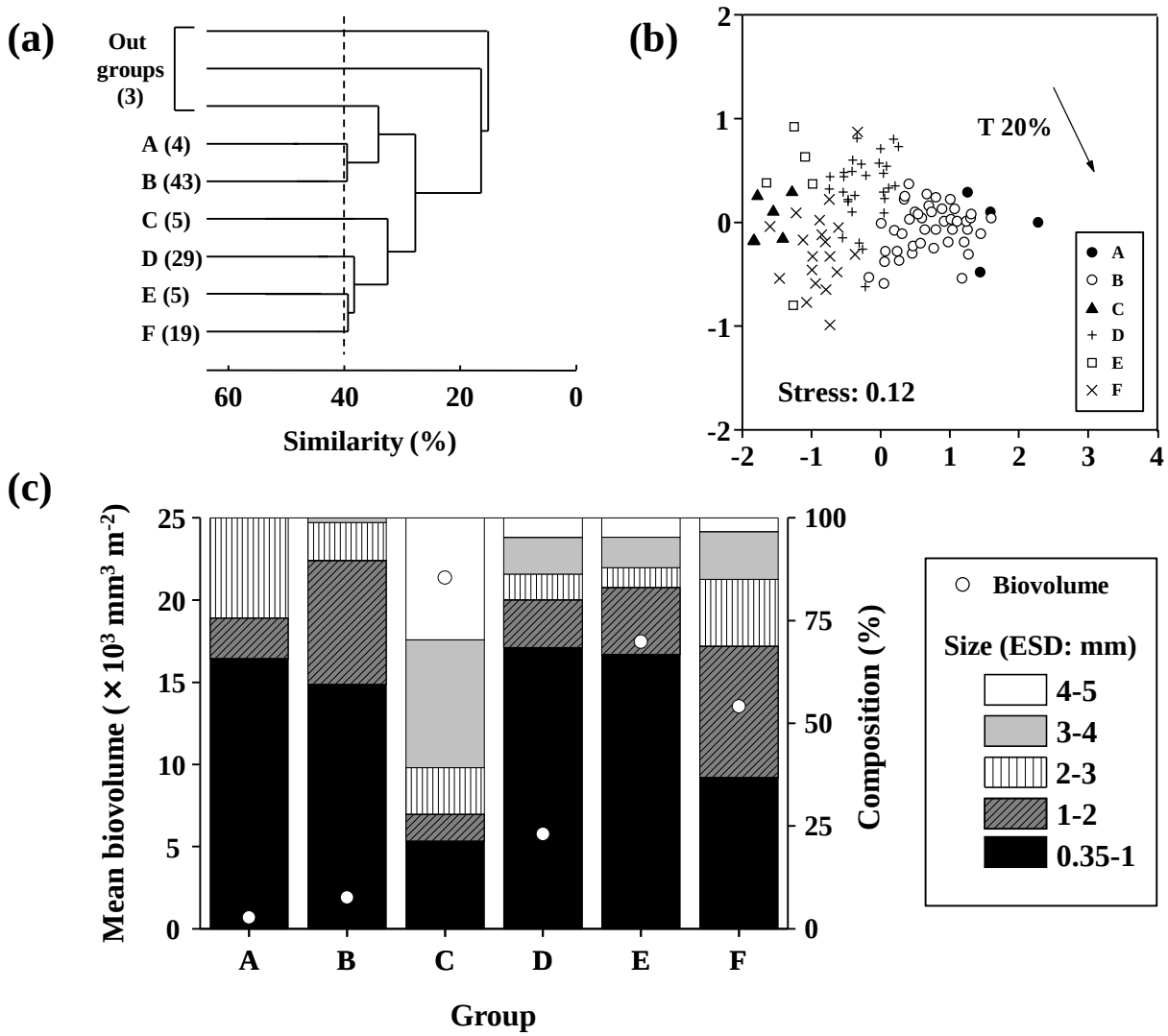

Fig. 5. (a) Results of cluster analysis based on mesozooplankton biovolume size spectra at Mombetsu harbor during 2011. Six groups (A–F) were identified at 40% Bray–Curtis similarity connected with UPGMA. Numbers in the parentheses indicate the number of dates each group contained. (b) NMDS plots of each group. The arrow and percentage indicate the direction of environmental parameters and the coefficient of determination (r^2), respectively. T: temperature. (c) Mean biovolume and size composition (ESD, mm) of each group.

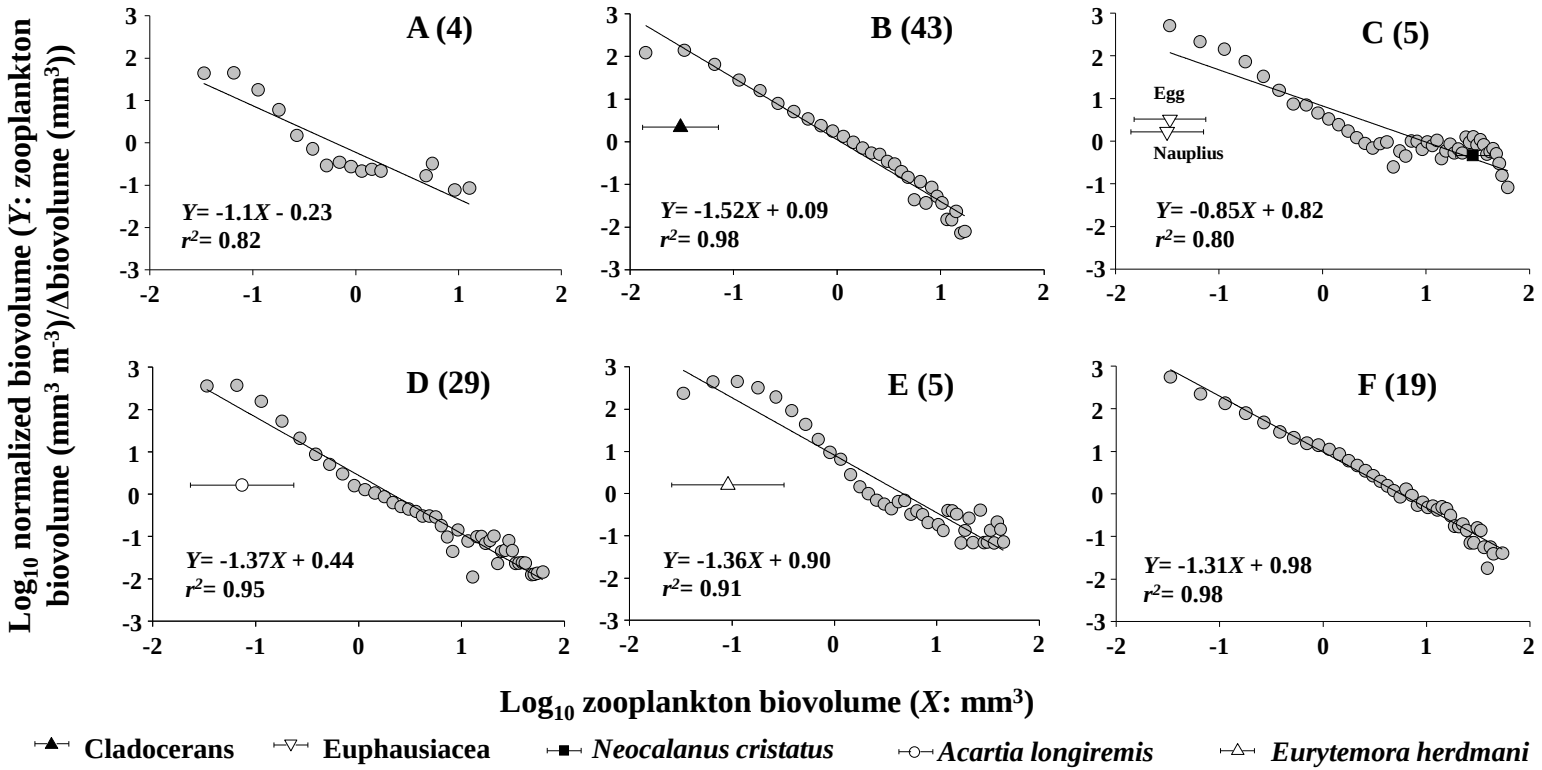

Fig. 6. Mean NBSS of six groups (A-F) identified from cluster analysis based on mesozooplankton biovolume size spectra at Mombetsu harbor from January to December 2011 (cf. Fig. 5). Numbers in the parentheses indicate the number of samples belonging to each group. For the dominant zooplankton species in each group (cf. Table 1), the mean (symbols) and standard deviation (bars) of the biovolume data are shown in the panel.

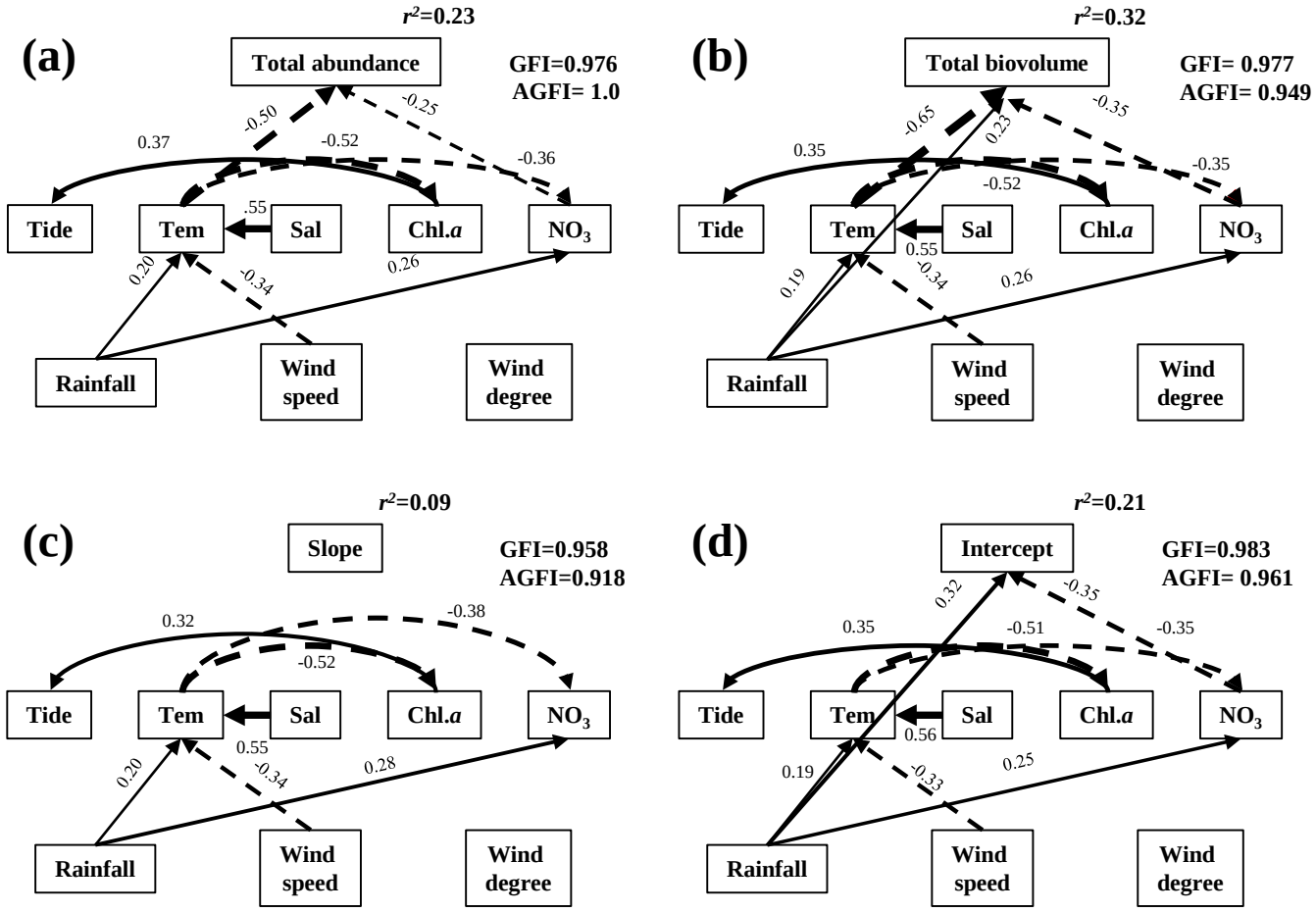

Fig. 7. Results of structural equation model (SEM) for total zooplankto (a) abundance and (b) biovolume and NBSS (c) slope and (d) intercept. The values along the pathways represent standardized path coefficients. Arrows with soild or dashed lines indicate positive or negative effects. The thicknesss of the arrows varies with the path coefficient values. The overall fit of the model was evaluated using the goodness-of-fit index (GFI) and the adjunct goodness-of-fit index (AGFI). Tide: daily differences of tidal level, Tem: sea temperature, Sal: salnity, Rainfall: daily amount of rainfall, Wind speed: daily maximum wind speed, Wind degree: daily maximum wind degree.

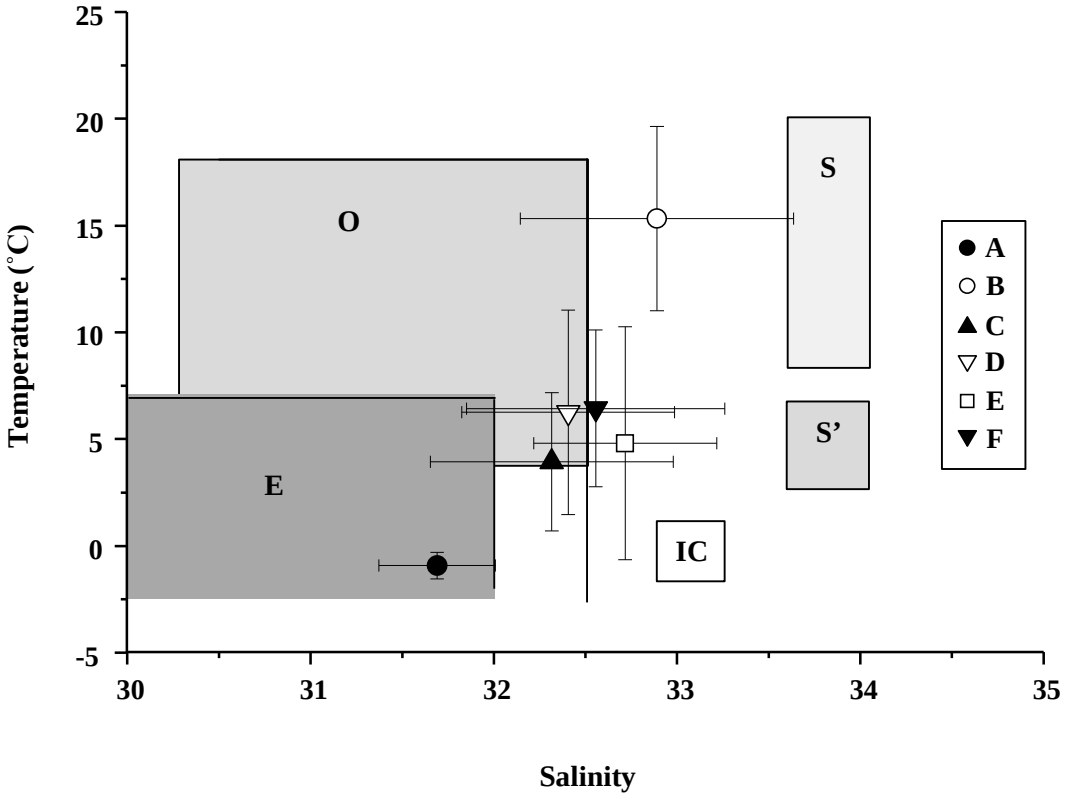

Fig. 8. T- S diagam of each zooplankton group observed period. Symbols and bars indicate means and standard deriations, respectively. Water mass classifications by Takizawa (1982) are shown in the panel. S: Soya Warm Water, S': Forerunner of Soya Warm Water, IC: Intermediate Cold Water, O: Okhotsk Surface Water, E: East Sakhalin Current Water.